

# Synthesis and dense kondo behavior of cubic AuBe<sub>5</sub>-type YbCu<sub>5</sub> compound — systematic change of physical properties in the YbCu<sub>5-x</sub>Ag<sub>x</sub> (0 ≤ x ≤ 1) system

K. Yoshimura<sup>a,\*</sup>, N. Tsujii<sup>a</sup>, J. He<sup>a</sup>, M. Kato<sup>a</sup>, K. Kosuge<sup>a</sup>, H. Michor<sup>b</sup>, K. Kreiner<sup>b</sup>, G. Hilscher<sup>b</sup>, T. Goto<sup>c</sup>

<sup>a</sup>Division of Chemistry, Graduate School of Science, Kyoto University, 606-01 Kyoto, Japan

<sup>b</sup>Institute für Experimentalphysik, Technische Universität Wien, Wiedner Hauptstrasse 8-10 / 131, A-1040 Wien, Austria

<sup>c</sup>Institute for Solid State Physics, the University of Tokyo, Roppongi, Tokyo 106, Japan

## Abstract

The cubic C15b (AuBe<sub>5</sub>) type YbCu<sub>5</sub> has been prepared for the first time in a single phase by a high-pressure apparatus. Its magnetic susceptibility, high field magnetization, specific heat and electric resistivity reveal that this compound belongs to the characteristic dense Kondo system. Preparation of cubic C15b (AuBe<sub>5</sub>) type YbCu<sub>5</sub> allowed us to discuss the physical properties of the pseudobinary system YbCu<sub>5-x</sub>Ag<sub>x</sub> in the whole composition region 0 ≤ x ≤ 1. © 1997 Elsevier Science S.A.

**Keywords:** Dense Kondo behavior; Phase diagram; YbCu<sub>5</sub>; YbCu<sub>5-x</sub>Ag<sub>x</sub>

## 1. Introduction

The cubic AuBe<sub>5</sub>-type (C15b type) Yb compound, YbCu<sub>5</sub>M (M = In, Pd, Au and Ag), is known to show a variety of distinct physical properties. YbCu<sub>5</sub>In exhibits an anomalous valence transition as a function of temperature and magnetic field, where localized moments of Yb<sup>3+</sup> at high temperatures and high magnetic fields collapse at low temperatures and low magnetic fields through the valence transition [1,2]. YbCu<sub>5</sub>Pd and YbCu<sub>5</sub>Au with stable localized moment Yb<sup>3+</sup> show transitions to anti-ferromagnetic long-range ordered state at low temperatures [3]. Furthermore, typical dense Kondo behavior is realized in YbCu<sub>5</sub>Ag; Yb<sup>3+</sup> localized moments stable at high temperatures are screened through the anti-parallel

coupling with conduction electron spins below the characteristic temperature called the Kondo temperature, which causes the enhanced Pauli paramagnetic state at low temperatures with a fairly large electronic specific heat coefficient,  $\gamma = 245 \text{ mJ mol}^{-1} \text{ K}^{-2}$ , i.e. large effective mass of conduction electrons [3]. These compounds are typical systems with which we can investigate the anomalous physical behaviors of 4f electrons in intermetallic compounds with respect to instability of localized moment of 4f elements, i.e. Kondo effect, which originated from hybridization of the 4f and conduction electrons.

Recently, we have been studying the pseudobinary systems, YbCu<sub>5-x</sub>Ag<sub>x</sub> [4] and YbCu<sub>5-x</sub>In<sub>x</sub> [5] as well as re-investigating the binary Yb–Cu system [6], and have found that the cubic YbCu<sub>5</sub> possesses the basic characters to investigate the C15b-type Yb system. Here, we report the recent success of synthesis of single phase C15b-type YbCu<sub>5</sub> as well as the prelimi-

\* Corresponding author.

nary result of re-investigation of the phase diagram of the Yb–Cu system in the Cu–YbCu<sub>3.5</sub> region, that we compare with the results of Iandelli and Palenzona [7]. We also report the systematic behaviors of the dense Kondo effect in the pseudobinary YbCu<sub>5-x</sub>Ag<sub>x</sub> in the whole composition range, combined with some published data [4].

## 2. Sample preparations and experimental procedures

The samples of YbCu<sub>5-x</sub>Ag<sub>x</sub> were prepared from 99.9% pure ytterbium, 99.99% pure copper and 99.999% pure silver metals by Ar arc-melting, followed by annealing in evacuated quartz tubes at 750°C for 10 days.

The samples of the binary Yb–Cu system were prepared by two kinds of preparation methods: the first one is similar to that used in the case of YbCu<sub>5-x</sub>Ag<sub>x</sub> system, and the second one is that the mixture of Yb (99.9% pure) and Cu (99.99% pure) were melted in evacuated quartz ampules by use of an electric furnace, followed by slow cooling at room temperature. Some of the samples thus prepared were treated under a pressure of 1.5 GPa at 900°C for 1 h by use of a piston-cylinder type high pressure apparatus.

The phase identification of the samples was performed by X-ray powder diffraction (XRPD), using Cu K<sub>α</sub> radiation. The metallographic texture was observed by scanning electron microscopy (SEM), and the chemical composition was analyzed by energy dispersive X-ray spectroscopy (EDX).

Magnetic susceptibility ( $\chi$ ) was measured by a superconducting quantum interface device (SQUID) magnetometer (Quantum Design, MPMS5). Electric resistivity ( $\rho$ ) was measured by the four-probe dc method. Although the absolute value of resistivity contains some error coming from inaccuracy in estimating the sample dimension, its error is at most 10%. Specific heat ( $C$ ) was measured by the adiabatic method utilizing a heat-pulse technique. High-field magnetization ( $M$ ) was measured by an induction method with well-balanced pickup coils. For this measurement, we used powdered specimens to exclude the eddy-current effect by pulsed field with duration time of 12 ms.

## 3. Results and discussion

X-ray powder diffraction patterns of YbCu<sub>5-x</sub>Ag<sub>x</sub> ( $0 \leq x \leq 1$ ) are shown in Fig. 1. In the composition region  $0.125 \leq x \leq 1.0$ , the samples are confirmed to crystallize in a single phase of the cubic AuBe<sub>5</sub>-type, while in the composition region  $0 \leq x \leq 0.125$ , the samples consist of two phase mixtures with the hexagonal CaCu<sub>5</sub>-type and the cubic AuBe<sub>5</sub>-type structures.

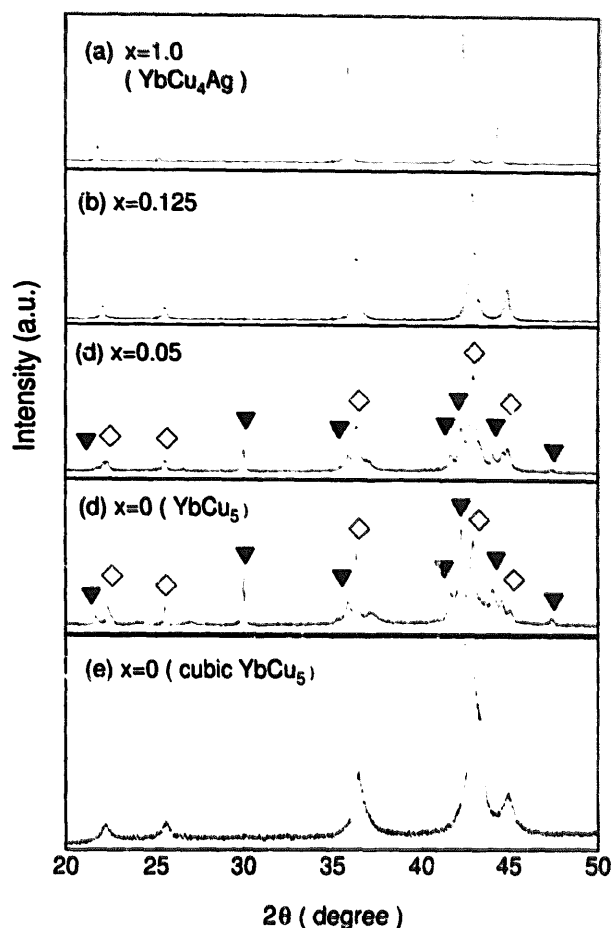


Fig. 1. X-ray powder diffraction patterns of YbCu<sub>5-x</sub>Ag<sub>x</sub> ( $x = 1.0, 0.125, 0.05$  and  $0$ ). The bottom pattern (e) shows that of the cubic YbCu<sub>5</sub> prepared under pressure.

As is shown below, the cubic AuBe<sub>5</sub>-type structure is the same as the structure of Yb<sub>2</sub>Cu<sub>9</sub>, which is a kind of modulated or super structure based on the cubic AuBe<sub>5</sub>-type structure [8]. The hexagonal CaCu<sub>5</sub>-type structure may be the same as the structure of Yb<sub>2</sub>Cu<sub>13</sub> [9], which is based on hexagonal CaCu<sub>5</sub>-type. As seen in Fig. 1, the XRPD pattern of YbCu<sub>5</sub> is very similar to that of YbCu<sub>4.95</sub>Ag<sub>0.05</sub>, which means that cubic AuBe<sub>5</sub>-type YbCu<sub>5</sub> is non-existent as asserted by Hornstra and Bushow [9]. Figure 2 shows that the XRPD pattern of nominal composition of YbCu<sub>5</sub> prepared under ambient pressure consists of that of Yb<sub>2</sub>Cu<sub>9</sub> phase [8] and Yb<sub>2</sub>Cu<sub>13</sub> phase [9] ('hexagonal YbCu<sub>5</sub>').

We have tried to re-examine the phase diagram of the Yb–Cu system in the composition region of Cu–YbCu<sub>3.5</sub> under ambient pressure. The main result is that in this composition range there exists only Yb<sub>2</sub>Cu<sub>13</sub>, Yb<sub>2</sub>Cu<sub>9</sub> and Yb<sub>2</sub>Cu<sub>7</sub> phases, each of which has some homogeneity composition range. The detail of the phase diagram study of the Yb–Cu system will be published elsewhere [10].

In order to elucidate the existence of YbCu<sub>5</sub> with

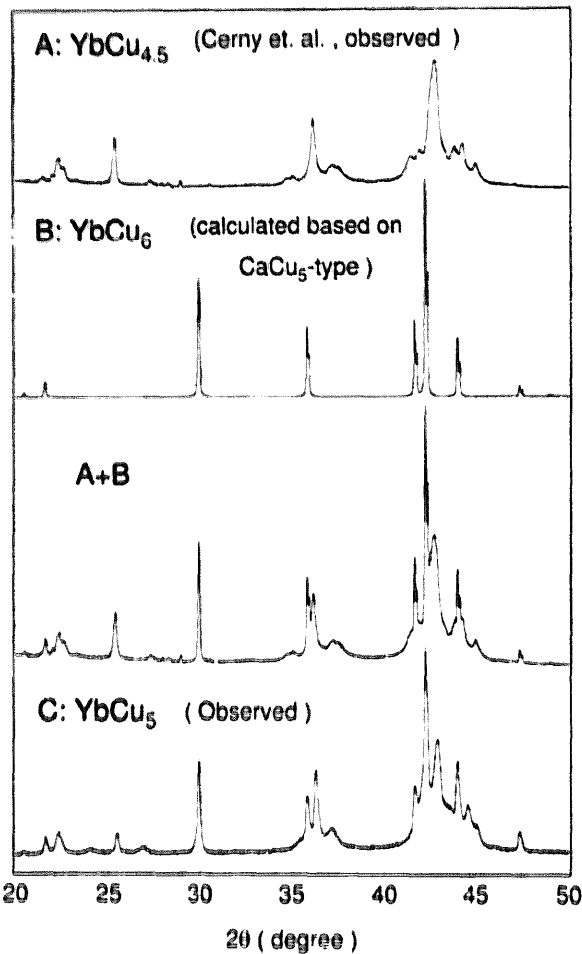


Fig. 2. X-ray powder diffraction patterns of the 'cubic YbCu<sub>5</sub>' (A), 'hexagonal YbCu<sub>5</sub>' (B), (A) + (B) and the prepared YbCu<sub>5</sub> (C) under ambient pressure.

the C15b type structure, we have treated the two phase mixtures YbCu<sub>5</sub> under a pressure of 1.5 GPa at 900°C for 1 h by use of a piston-cylinder type high pressure apparatus. The sample was encapsulated in a boron nitride container, which was inserted into the cylindrical carbon heater. Pyrophyllite block was used as a pressure-transmitting medium. The sample obtained was subsequently annealed in an evacuated quartz tube at 350°C for 2 weeks. The XRPD pattern shows a single phase of C15b-type as seen in Fig. 1 (bottom). Each peak of the XRPD spectrum is wider than that of the other sample. This may be caused by the stacking fault along the [111] direction. The difference in stacking along [111] is an essential factor of determining the cubic AuBe<sub>5</sub>-type and the hexagonal CaCu<sub>5</sub>-type structures from each other. Since the difference of free energy of cubic- and hexagonal-YbCu<sub>5</sub> may be very small, it is not so strange that stacking faults are involved in YbCu<sub>5</sub>. Composition of the sample was confirmed to be almost the same composition as the nominal composition (YbCu<sub>5</sub>) by

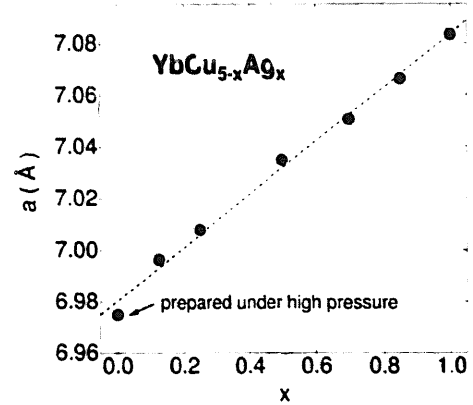


Fig. 3. Lattice parameter  $a$  (Å) vs.  $x$  of the cubic YbCu<sub>5-x</sub>Ag<sub>x</sub>.

EDX measurement. It is also noted that the samples with the composition YbCu<sub>6.0</sub>-YbCu<sub>8.0</sub> (the phase is 'hexagonal YbCu<sub>5</sub>' or 'hexagonal YbCu<sub>5</sub>' + Cu under ambient pressure) show the phase transition to the cubic AuBe<sub>5</sub>-type YbCu<sub>5</sub> + Cu under high pressure.

In Fig. 3 is plotted against  $x$  the lattice parameter  $a$  in YbCu<sub>5-x</sub>Ag<sub>x</sub>, determined from XRPD patterns by means of the Wilson-Pike deviation function calculating method, which shows a systematic change linear with  $x$ , i.e. the Vegard's law. These results indicate that the cubic YbCu<sub>5</sub> with AuBe<sub>5</sub>-type structure has been successfully prepared as a single phase by high-pressure synthesis.

Figure 4 shows the temperature ( $T$ ) dependence of magnetic susceptibility ( $\chi$ ) of YbCu<sub>5-x</sub>Ag<sub>x</sub>. The broad maximum around  $T_{\max}$  of 40 K for  $x = 1$  shifts systematically to lower temperatures and is still observed for  $x = 0$  around  $T_{\max}$  of 10 K. The value of  $\chi$  of the cubic YbCu<sub>5</sub> ( $x = 0$ ) at  $T_{\max}$  is larger than that of 'the hexagonal YbCu<sub>5</sub>' by a 10<sup>6</sup> factor. At temperatures moderately higher than  $T_{\max}$ , the Curie-Weiss behavior is observed for all the sample. From the Curie constant an effective moment ( $\mu_{\text{eff}}$ ) of 4.4–4.6  $\mu_{\text{B}}$  Yb<sup>-1</sup> is obtained, and is independent of  $x$ , which agrees well with  $\mu_{\text{eff}} = 4.54 \mu_{\text{B}}$  for  $J = 7/2$  and  $g_J = 8/7$  for Yb<sup>3+</sup> free ion. This is completely in contrast to the case of 'the hexagonal YbCu<sub>5</sub>' in which Yb is in a divalent state and is completely non-magnetic. As seen in Fig. 4, the value of  $\chi$  tends to be constant at low temperatures  $\chi(0)$ , suggesting the sample comes to the Fermi liquid state with a large enhancement of  $\chi(0)$ . These results of YbCu<sub>5-x</sub>Ag<sub>x</sub> are common with the dense Kondo and the heavy Fermion systems: Yb<sup>3+</sup> localized moments stable at high temperatures come to collapse and delocalize by screening effect coupled with conduction electron spins below the characteristic temperature called Kondo temperature ( $T_K$ ), which is proportional to  $T_{\max}$ . Therefore, the  $T_K$  shifts systematically to lower temperature with decreasing  $x$  in

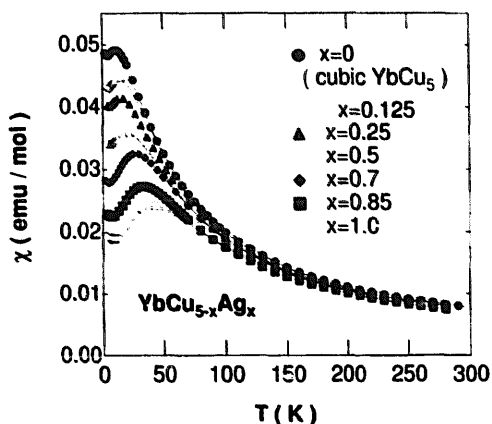


Fig. 4. Temperature dependence of magnetic susceptibility ( $\chi$ ) of the cubic  $\text{YbCu}_{5-x}\text{Ag}_x$ .

$\text{YbCu}_{5-x}\text{Ag}_x$ . Our results have been found to agree well with the Coqblin–Schrieffer thermodynamic model [11] in the whole composition range [4,12].

High-field magnetization curves obtained at 1.6 K and 4.2 K are shown in Fig. 5. The broad metamagnetic-like behavior was observed around 18 T for  $x=0$ . With increasing  $x$ , this behavior takes place in the higher magnetic fields. Similar metamagnetic field dependence of magnetization have been reported in some Ce, Yb and U compounds [13–15]. This behavior has been theoretically predicted for the dense Kondo system from the calculation based on the Coqblin–Schrieffer model when a level crossing occurs between low-lying states split by the crystalline field [16,17]. This result also indicates that the present pseudobinary system belongs to the dense Kondo system in which  $T_K$  changes systematically with the composition  $x$ .

In Fig. 6,  $C/T$  is plotted against  $T^2$ . No upturn behavior was observed except for a small anomaly at 2.2 K due to the anti-ferromagnetic transition of small amount of the possible impurity of  $\text{Yb}_2\text{O}_3$ , suggesting that no magnetic order exists in this system even at

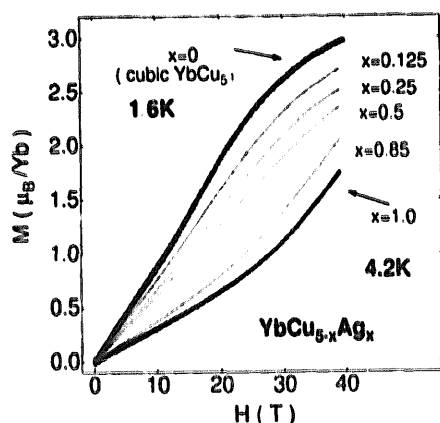


Fig. 5. High field magnetization curves of the cubic  $\text{YbCu}_{5-x}\text{Ag}_x$  at 1.6 K for  $x=0$  and at 4.2 K for  $x=1.0, 0.85, 0.5, 0.25$  and  $0.125$ .

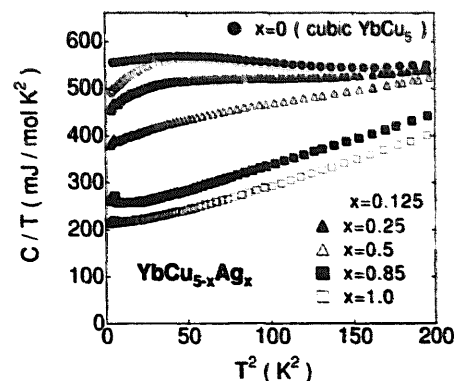


Fig. 6. Temperature dependence of specific heat ( $C$ ) of the cubic  $\text{YbCu}_{5-x}\text{Ag}_x$ .  $C/T$  is plotted against  $T^2$ .

low temperatures. This value of  $C/T$  is substantially enhanced in comparison with that for free electron system. The electronic specific heat coefficient,  $\gamma$ , estimated by extrapolation of  $T$  to 0 in the  $C/T$  vs.  $T^2$  curves, increases systematically from  $210 \text{ mJ mol}^{-1} \text{ K}^{-2}$  for  $x=1.0$ – $550 \text{ mJ mol}^{-1} \text{ K}^{-2}$  for  $x=0$ , implying that the effective mass of conduction electrons is fairly heavy due to the hybridization between 4f and conduction electrons. The cubic C15b  $\text{YbCu}_5$ , therefore, can be regarded as one of the heaviest electron systems among the Yb intermetallics. Details of analyses will also be presented elsewhere [12].

In Fig. 7 is shown the electric resistivity ( $\rho$ ) normalized by that at 273 K as a function of temperature in semi-logarithmic plots. The value of  $\rho$  exhibits characteristic temperature dependence and changes systematically with  $x$ . At high temperatures,  $\rho$  shows a metallic temperature dependence. Then, with decreasing temperature,  $\rho$  has a broad minimum, increases gradually in a logarithmic way, makes a broad maximum and again decreases very sharply. This behavior has been observed in many dense Kondo systems. The last rapid decrease of  $\rho$  is possibly due to the Kondo-lattice formation, suggesting the realization of the Fermi liquid state at low temperatures. The resistivity is replotted as  $\{\rho(T) - \rho(0)\} / \{\rho(273 \text{ K}) - \rho(0)\}$  vs.  $T$  in a logarithmic scale for both  $x$  and  $y$  axes in Fig. 8, where  $\rho(0)$  is the residual resistivity. One can see that the slope of these graphs is 2 at low temperatures, which is led to the relation:  $\{\rho(T) - \rho(0)\} = AT^2$ , where  $A$  is a coefficient, indicating the system is in a Fermi liquid state at low temperatures. This situation is completely consistent with the above results of  $\chi$ , high-field  $M$  and  $C$ . The coefficient  $A$  between  $\{\rho(T) - \rho(0)\}$  and  $T^2$  is correlated universally with the value of  $\gamma$  through the correlation with  $T_K$  in the case of Fermi liquid systems [18]. This relation has been found to be valid in this system. Details have been reported elsewhere [4]. All these results imply that the present system, including the

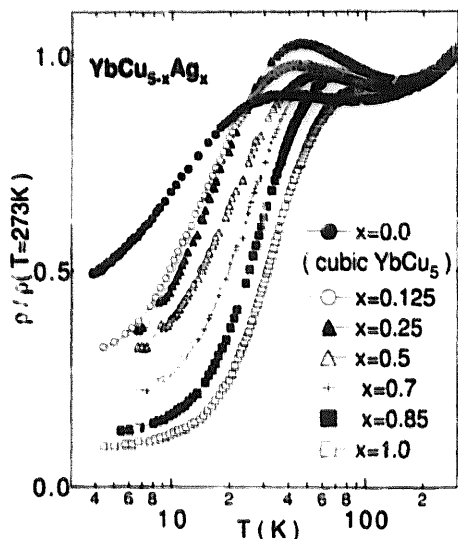


Fig. 7. Temperature dependence of electric resistivity ( $\rho$ ) of the cubic  $\text{YbCu}_{5-x}\text{Ag}_x$ . The value of  $\rho$  is normalized at 273 K [ $\rho(T=273\text{ K})$ ].

cubic C15b  $\text{YbCu}_5$ , is in a Fermi liquid state at low temperatures. Furthermore, the composition dependence of  $A$  could be successfully explained in terms of chemical pressure, that is, when Ag with larger metallic radius is substituted by Cu with smaller metallic radius in  $\text{YbCu}_4\text{Ag}$ , the lattice feels negative pressure [4,12], referring to the previous results of pressure dependence of resistivity of  $\text{YbCu}_4\text{Ag}$  [19,20].

#### 4. Conclusion

Single phase of the cubic C15b ( $\text{AuBe}_5$ ) type  $\text{YbCu}_5$  has been successfully prepared by high-pressure synthesis. Its magnetic susceptibility shows a maximum around 10 K, above which it shows the Curie-Weiss law with the effective moment of  $\text{Yb}^{3+}$ , and below which it tends to be constant at low temperatures. The high-field magnetization at 1.6 K shows a metamagnetic-like behavior. The electric resistivity follows the  $T^2$  dependence at low temperatures, which agrees with the Fermi liquid state at low temperatures. The electronic specific heat coefficient,  $\gamma$ , was measured to be approximately  $550\text{ mJ mol}^{-1}\text{ K}^{-2}$ , which indicates very heavy effective mass of conduction electrons. These results can be explained assuming typical dense Kondo behaviors as predicted from the Coqblin-Schrieffer thermodynamical model.

The samples of the pseudobinary  $\text{YbCu}_{5-x}\text{Ag}_x$  system prepared in a single phase of the cubic C15b ( $\text{AuBe}_5$ ) type for  $0 \leq x \leq 1$  has been found to show the systematic and characteristic physical properties of the dense Kondo system, in which the Kondo temperature  $T_K$  shifts to higher temperature with increasing  $x$ .

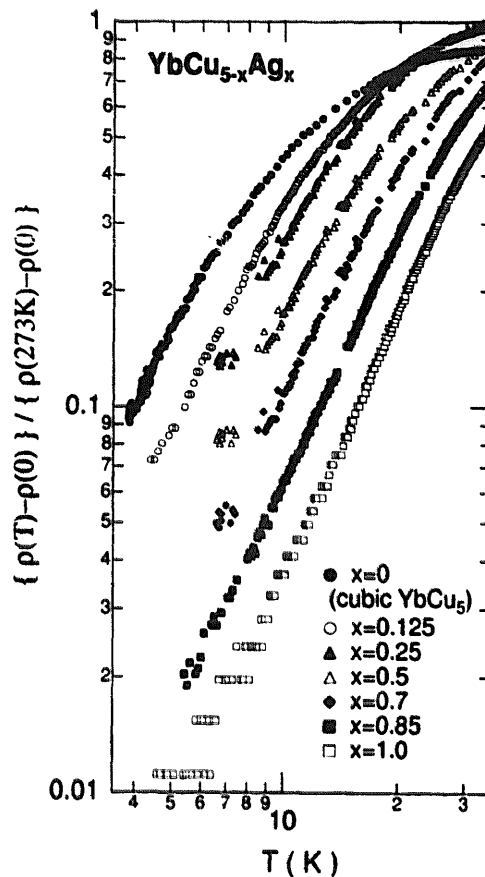


Fig. 8.  $\text{Log}\{[\rho(T) - \rho(0)] / [\rho(273\text{ K}) - \rho(0)]\}$  vs.  $\text{log } T$  curves of the cubic  $\text{YbCu}_{5-x}\text{Ag}_x$ .

#### Acknowledgements

The authors wish to thank F. Amita and M. Nakanishi for assistance and discussion in high pressure synthesis, and also to S. Aoyagi and A. Isono of JEOL for SEM and EDX measurements.

#### References

- [1] I. Felner, I. Novik, Phys. Rev. B 33 (1986) 617.
- [2] K. Yoshimura, T. Nitta, M. Mekata, et al., Phys. Rev. Lett. 60 (1988) 851.
- [3] C. Rossel, K.N. Yang, M.B. Maple, Z. Fisk, E. Zirngiebl, J.D. Thompson, Phys. Rev. B 35 (1987) 1914.
- [4] N. Tsujii, J. He, K. Yoshimura, et al., Phys. Rev. B 55 (1997) 1032.
- [5] J. He, N. Tsujii, K. Yoshimura, K. Kosuge, T. Goto, J. Phys. Soc. Jpn. 66 (1997) 2481.
- [6] J. He, N. Tsujii, M. Nakanishi, K. Yoshimura, K. Kosuge, J. Alloy. Comp. 240 (1996) 261.
- [7] A. Iandelli, A. Palenzona, J. Less-Common Met. 25 (1971) 333.
- [8] R. Cerny, M. François, K. Yvon, et al., J. Phys. Condens. Matter 8 (1996) 446.
- [9] J. Hornstra, K.H.J. Buschow, J. Less-Common Met. 27 (1972) 123.

- [10] in preparation
- [11] V.T. Rajan, *Phys. Rev. Lett.* 51 (1983) 308.
- [12] N. Tsujii, J. He, F. Amita, K. Yoshimura, K. Kosuge, H. Michor, G. Hilscher, T. Goto, *Phys. Rev. B* 56 (1997) in press.
- [13] J.M. Mignot, J. Flouquet, P. Haen, F. Lapiere, L. Puech, J. Voiron, *J. Mag. Mag. Mater.* 76–77 (1988) 97.
- [14] G. van Kalkeren, H. van Nassou, F.R. de Boer, *J. Mag. Mag. Mater.* 47–48 (1985) 105.
- [15] J. Flouquet, P. Haen, F. Lapiere, D. Jaccard, G. Remenyi, *J. Mag. Mag. Mater.* 54–57 (1986) 322.
- [16] A.C. Hewson, J.W. Rasul, *J. Phys. C: Solid State Phys.* 16 (1983) 6799.
- [17] N. Kawakami, A. Okiji, *Phys. Lett.* 103A (1984) 205.
- [18] A. Yoshimori, H. Kasai, *J. Mag. Mag. Mater.* 31–34 (1983) 475.
- [19] E. Bauer, R. Hauser, E. Grantz, K. Payer, G. Oomi, T. Kagayama, *Phys Rev. B* 48 (1993) 15873.
- [20] T. Graf, J.M. Lawrence, M.F. Hundley, et al., *Phys Rev. B* 52 (1995) 3099.